Critical Point of a 2D Ising Honeycomb Lattice in Zero External Field

Rishav Koirala, Haotian Song

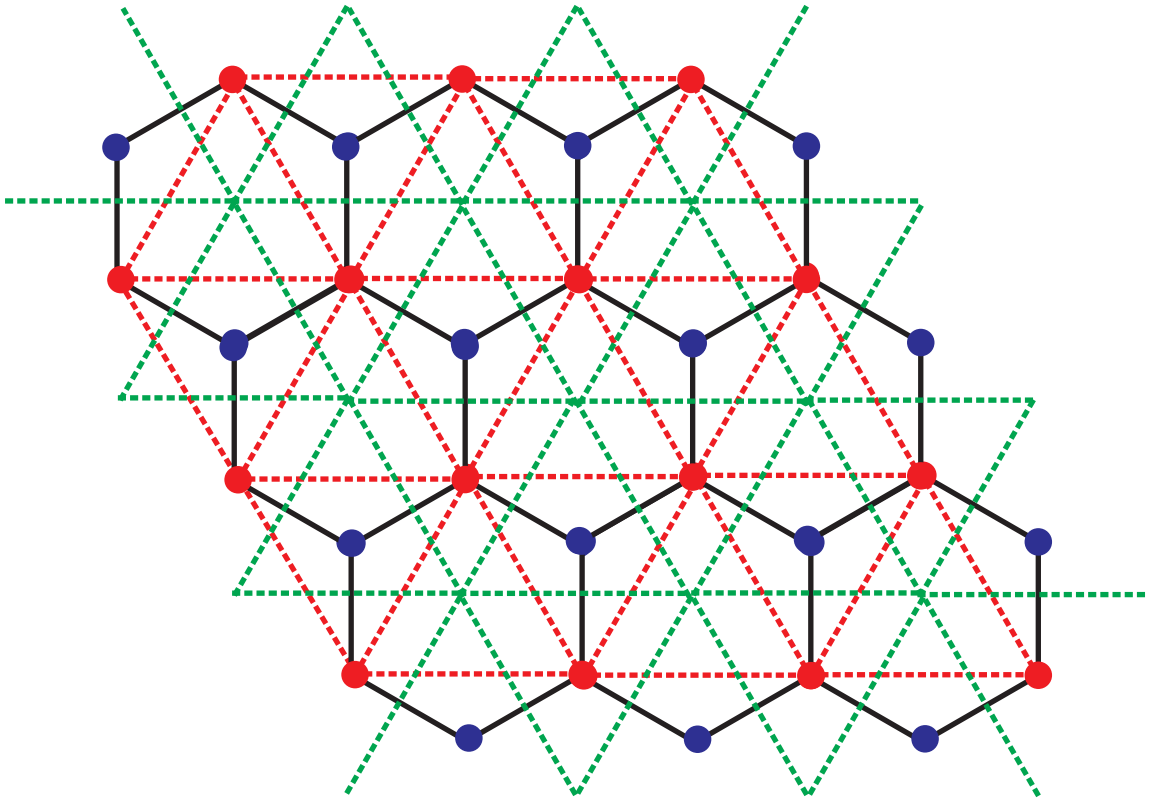

Submitted March 27, 2023

Project Report
PC5202 Advanced Statistical Mechanics

Contents

List of Figures

List of Tables

Abstract

After the famous 2D square Ising lattice, the hexagonal lattice or honeycomb is the next simplest planar geometry. Like the square lattice, the honeycomb displays a phase transition from a non-magnetic or disordered state to a ferromagnetic state with some residual magnetism. In the first part of this report, we derive the critical point of the honeycomb in zero external field from the ideas of duality and the Star-Triangle Transformation. In the latter part, we discuss our results of a Monte-Carlo simulation on the honeycomb and the numerical evidence of the critical point based on the divergences of the specific heat and magnetic susceptibility. Finally, we explore in our simulation the effects of defects in the honeycomb in cases where the lattice has impurities or missing spins, and observe how the critical point shifts as a consequence.

1 Introduction

The honeycomb lattice in two dimensions is a net of interconnected spins arranged in a hexagonal pattern, resembling a honeycomb. Each vertex i contains an Ising-type spin ($\sigma_i = \pm 1/2$) interacting with three other spins at the three adjoining vertices of the lattice. The honeycomb is the second simplest net in two dimensions after the square lattice. It is a

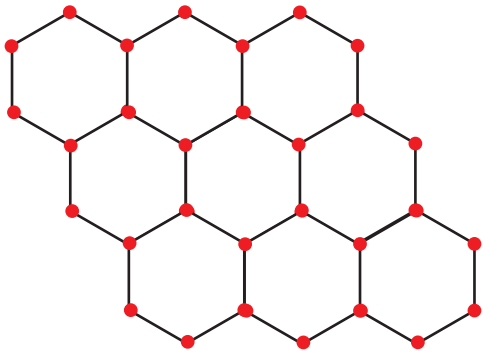

Figure 1: A portion of the honeycomb lattice with spins colored in red at the vertices. The lattice extends indefinitely in all directions to negate boundary effects.

geometry of significant interest, since several important natural substances form hexagonal structures – for example, graphene. Just like the square lattice, the honeycomb undergoes a phase transition at a particular critical temperature, where second-order properties like the specific heat and the magnetic susceptibility diverge.

In our report, we explore this critical point using two methods. First, we use the arguments of duality we learned in class combined with another idea called the Star-Triangle Transformation to derive the critical point theoretically. Then, in the second part, we run a computer simulation of a finite-size honeycomb and derive the critical point, verifying it against the expected result.

Lastly, we turn to a "defective" honeycomb lattice, where some lattice sites are missing (holes) or have impurities that double the interaction strength with neighboring spins, and see how the critical point shifts as the number of holes or impurities is changed.

2 Analytical Solution

[1]

The Hamiltonian of an arbitrary field-free 2D Ising lattice with spins $\sigma_i = \pm 1/2$ can be

[1] This section is an elaboration on the derivations of Strečka and Jaščur, 2015 and Baxter, 1989.

written as

$$H = -J \sum_{\langle i,j \rangle}^{N_B} \sigma_i \sigma_j. \tag{1}$$

The sum here runs over all nearest-neighbor pairs $\langle i, j \rangle$. The number N_B is the number of such pairs in the lattice. It is useful to think of each interaction pair as forming a "bond", in which case N_B can be interpreted simply as the number of bonds. If each spin in a lattice of N spins has q neighbors, then it can be shown that $N_B = qN/2$ as long as boundary conditions are ignored (valid in the thermodynamic limit). For example, the honeycomb lattice has $q = 3$, so with $N = 100$ spins, there are 150 bonds in the lattice. The interaction strength $J > 0$ denotes ferromagnetic coupling.

The partition function of the lattice is

$$Z = \sum_{\{\sigma_i\}} \exp\left(-\beta H\right) = \sum_{\{\sigma_i\}} \exp\left(K \sum_{\langle i,j \rangle}^{N_B} \sigma_i \sigma_j\right), \tag{2}$$

where $\beta = 1/(k_B T)$ and $K \equiv \beta J$. This sum counts all possible combinations of spin values in the lattice.

2.1 Different Representations of the Partition Function

We saw in class that the partition function can be rewritten in two equivalent forms that highlight its significance in the regimes of high temperatures ($\beta << 1$) and low temperatures ($\beta >> 1$). These two forms also have different, yet related, geometric interpretations.

2.1.1 High Temperature Series Expansion

First, we note that, since $\sigma_i \sigma_j = \pm 1/4$, the term $\exp\left(K \sigma_i \sigma_j\right)$ can be written as

$$\exp\left(K\sigma_i\sigma_j\right) = \cosh\left(\frac{K}{4}\right) + 4\sigma_i\sigma_j \sinh\left(\frac{K}{4}\right) = \cosh\left(\frac{K}{4}\right)\left(1 + 4\sigma_i\sigma_j \tanh\left(\frac{K}{4}\right)\right). \tag{3}$$

Substituting this in (2) we get

$$Z = \cosh\left(\frac{K}{4}\right)^{N_B} \sum_{\{\sigma_i\}} \prod_{\langle i,j \rangle} \left(1 + 4\sigma_i\sigma_j \tanh\left(\frac{K}{4}\right)\right). \tag{4}$$

This representation has an interesting geometric interpretation. If each inner product $\sigma_i \sigma_j$ can be thought of as a bond, the outer product, on expansion, yields different terms in powers of $\tanh(K/4)$, whose pre-factor is the product of spins $4^n(\sigma_i\sigma_j) \cdot (\sigma_j\sigma_k) \cdots$. When summed over all spin-configurations $\{\sigma_i\}$, a particular $\tanh^p(K/4)$ term will vanish unless

the pre-factor product of spins has each spin in the product occurring an *even* number of times. In terms of bonds, this translates to forming a *closed* loop or a *polygon* on the lattice.

As discussed in class, for a square lattice, the first non-vanishing term in the product expansion is $\tanh^4(K/4)$, which corresponds to a square loop covering four spins – the smallest "unit" of that lattice. Similarly, for a honeycomb lattice, the first such term is $\tanh^6(K/4)$, corresponding to the smallest polygon possible to be drawn on the lattice. Each non-vanishing contribution to Z thus has the pre-factor $4^p(\sigma_i\sigma_j)\cdot(\sigma_j\sigma_k)\cdots = 1$ necessarily. The partition function is then

$$Z = 2^N \cosh\left(\frac{K}{4}\right)^{N_B} \sum_{\text{polygons}} \left(\tanh\frac{K}{4}\right)^p . \tag{5}$$

Here, p refers to the number of "sides" in a polygon made on the lattice, and the summation is over all possible polygons. As $T \to \infty$, $K \to 0$, so the above expansion is particularly useful at high temperatures; this is the *high temperature series expansion*.

2.1.2 Low Temperature Series Expansion

Yet another way to rewrite Z is to first consider the "ground state" of the lattice, where all the spins are aligned in a particular way, either $+1/2$ or $-1/2$. Then, for other states, we can focus on the number of "misaligned" or unlike spin pairs and look at how they change the ground state energy. The Hamiltonian (1) from this perspective is

$$H = -\frac{N_B J}{4} + J\sum_{\langle i,j\rangle}\left(\frac{1}{4} - \sigma_i\sigma_j\right). \tag{6}$$

The first term in the above corresponds to the energy in the ground state. In the second term, the summation counts the number of spin pairs, where each unlike spin pair contributes an energy $J/2$ to the Hamiltonian, and each like spin pair contributes nothing. The partition function can then be recast as

$$Z = \exp\left(\frac{KN_B}{4}\right)\sum_{\{\sigma_i\}}\exp\left(-p\frac{K}{2}\right), \tag{7}$$

where p is the number of unlike bond pairs in the lattice.

The geometrical interpretation of this representation requires looking at the *dual* of the lattice. The dual lattice is constructed by bisecting the edges of the original lattice and imagining a spin located at the point of intersection of the bisectors – each intersection point is a vertex of the dual lattice. In class, we saw that the square lattice is self-dual, meaning the dual lattice is also a square lattice. On the other hand, the dual lattice of the honeycomb is a triangular lattice, as can be seen in Figure 2. Now, we want to figure out how many spins or vertices N_D are located in the dual lattice if the original lattice has N

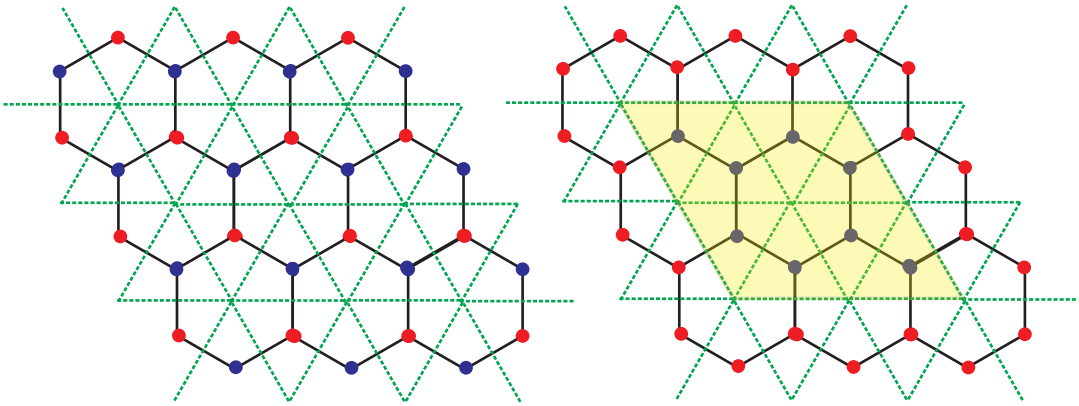

Figure 2: **[Left]** The dual of the honeycomb lattice is a triangular lattice (green). **[Right]** A domain (shaded yellow region) containing 8 spins. The blue and the red vertices are unlike spins.

spins or vertices. If N_B is the number of bond-pairs in the original lattice, it can be shown mathematically that, in the limit of large N,

$$N + N_D = N_B. \tag{8}$$

Since we know $N_B = qN/2$ and $q = 3$ for a honeycomb lattice, we obtain $N_D = N/2$ for the triangular lattice. In other words, the lattice dual to the honeycomb has *half* the number of spins as the honeycomb.

Now, for an arbitrary spin configuration in the honeycomb, we can construct a figure on the dual lattice as follows:

1. We superimpose the dual triangular lattice with dotted lines over the honeycomb.
2. If two neighboring spins are unlike, then we draw a solid line over the edge of the dual lattice passing between those spins.
3. If the spins are like, we do nothing.

In this fashion, we make sub-graphs on the dual lattice graph. These are essentially *domains* – polygons separating the $+1/2$ spins from the $-1/2$ spins. Moreover, these domains do not change if we apply the transformation $\sigma_i \to -\sigma_i$ on the lattice (i.e. reverse all spins). All this taken into account, we can write down Z as

$$Z = 2\exp\left(\frac{KN_B}{4}\right) \sum_{\text{polygons}} \exp\left(-p\frac{K}{2}\right), \tag{9}$$

where the sum now runs over all possible domains we can draw on the dual lattice for all possible spin configurations of the original lattice. The variable p, earlier used to denote the number of unlike spin pairs, is now the number of sides to each domain sub-graph. The factor of 2 takes care of the spin-flip geometry discussed earlier, but it does not matter

in the thermodynamic limit. As $T \to 0$, $K \to \infty$, so this representation is well-suited for approximating low-temperature cases; this is the *low temperature series expansion*.

2.2 Duality

The two representations of Z discussed in the previous section are different in the sense that the summations are performed over polygons in different lattices: one in the original lattice itself, and the other in the dual lattice. Nevertheless, they are exact and equivalent if one performs the summation in the thermodynamic limit $N \to \infty$. Looking at each pair of corresponding terms in the summations in (5) and (9), we note that, if

$$\exp\left(-\frac{K_D}{2}\right) = \tanh\left(\frac{K}{4}\right), \text{ then} \tag{10}$$

$$\frac{Z(N_D, K_D)}{\exp\left(\frac{K_D N_B}{4}\right)} = \frac{Z(N, K)}{2^N \left(\cosh\left(\frac{K_D}{4}\right)\right)^{N_B}}. \tag{11}$$

Here, the subscript D refers to the dual lattice (and the low temperature series expansion of Z). The variable $K_D = \beta_D J$. These two equations can be combined together after some algebra to highlight the symmetry between a lattice and its dual:

$$\frac{Z(N_D, K_D)}{\left(2\sinh\left(\frac{K}{2}\right)\right)^{N/2}} = \frac{Z(N, K)}{\left(2\sinh\left(\frac{K_D}{2}\right)\right)^{N_D/2}}. \tag{12}$$

This duality relation establishes a correspondence between the high temperature model of the partition function of a lattice and the low temperature model of the partition function of the dual lattice.

The symmetry between a lattice and its dual can be highlighted further by rewriting Equation 10 in a more symmetric form:

$$\sinh\left(\frac{K}{2}\right)\sinh\left(\frac{K_D}{2}\right) = 1. \tag{13}$$

For the special case of a square lattice, which is self-dual ($Z(N_D, K_D) = Z(N, K)$ and $N_D = N$), if there is a critical point K^* on the main lattice, it must also be the critical point (K_D^*) in the dual lattice: $K^* = K_D^*$. Using this fact in (13), we readily obtain

$$\sinh^2\left(\frac{K^*}{2}\right) = 1 \implies T^* \simeq 0.567296\,\frac{J}{k_B}, \tag{14}$$

which is the critical temperature for a 2D spin-1/2 square lattice.

For other geometries like the honeycomb, unfortunately, this simple idea does not work, since the lattices are *not* self-dual – i.e., $Z(N, K) \neq Z(N_D, K_D)$. In other words, if there is a critical point K^* in a lattice, there will be a different K_D^* in the dual lattice, where $K^* \neq K_D^*$. Thus, we cannot use Equation 13 to extract the critical temperature.

2.3 The Star-Triangle Transformation

In order to overcome this problem, we need another trick – something that maps the high temperature model of Z on a lattice to the low temperature model of Z on the *same* lattice.

To arrive there, first we note that the honeycomb lattice is *bipartite*. This means it can be decomposed into two disjoint sub-lattices, where no two vertices in the same sub-lattice are nearest neighbors of each other. In the case of a honeycomb, this is achieved by picking a hexagonal unit cell in the lattice and giving every alternate vertex of it a second color. In Figure 3, all the red vertices belong to one triangular sub-lattice, say $\mathcal{A}$, whereas all the blue vertices belong to a second triangular sub-lattice, $\mathcal{B}$. Since the two sub-lattices are disjoint, we can sum over the spin degrees of freedom in either sub-lattice independently of the other (the spins in a sub-lattice do not interact with each other). It makes sense to write down the full Hamiltonian as a sum over the various site Hamiltonians:

$$H = \sum_{i \in \mathcal{B}}^{N} H_i, \tag{15}$$

where

$$H_i = -J\sigma_i^{\mathcal{B}} \left(\sigma_j^{\mathcal{A}} + \sigma_k^{\mathcal{A}} + \sigma_l^{\mathcal{A}}\right). \tag{16}$$

Here, each $\sigma_i^{\mathcal{B}}$ corresponds to a spin in $\mathcal{B}$ (blue) interacting with three spins $\sigma_j^{\mathcal{A}}, \sigma_k^{\mathcal{A}}$, and $\sigma_l^{\mathcal{A}}$ in $\mathcal{A}$ (red). In this picture, we can rewrite the partition function of the honeycomb as

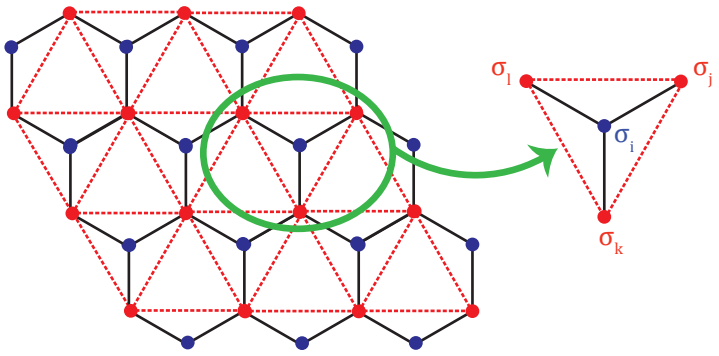

Figure 3: **[Left]** The honeycomb as a bipartite lattice. Spins colored blue form one sub-lattice $\mathcal{B}$, and those colored red form another sub-lattice, $\mathcal{A}$. **[Right]** Each spin σ_i of $\mathcal{B}$ interacts with three spins in $\mathcal{A}$.

$$Z = \sum_{\{\sigma_j^{\mathcal{A}}\}} \prod_{i=1}^{N} \sum_{\sigma_i^{\mathcal{B}} = \pm 1/2} \exp\left(K\sigma_i^{\mathcal{B}} \left(\sigma_j^{\mathcal{A}} + \sigma_k^{\mathcal{A}} + \sigma_l^{\mathcal{A}}\right)\right), \tag{17}$$

where the outer sum is carried out over all the possible spin configurations in $\mathcal{A}$. The product goes through all the spins in $\mathcal{B}$, and the inner sum adds up the two spin-states for

each spin in $\mathcal{B}$. The advantage of this picture is that each spin $\sigma_i^{\mathcal{B}}$ appears only *once* in the product. This means we can perform the inner sum immediately over its spin-states:

$$\sum_{\sigma_i^{\mathcal{B}}=\pm 1/2} \exp\left(K\sigma_i^{\mathcal{B}}\left(\sigma_j^{\mathcal{A}}+\sigma_k^{\mathcal{A}}+\sigma_l^{\mathcal{A}}\right)\right) = 2\cosh\left[\frac{K}{2}\left(\sigma_j^{\mathcal{A}}+\sigma_k^{\mathcal{A}}+\sigma_l^{\mathcal{A}}\right)\right]. \tag{18}$$

Now comes the main idea. We argue that,

$$2\cosh\left[\frac{K}{2}\left(\sigma_j^{\mathcal{A}}+\sigma_k^{\mathcal{A}}+\sigma_l^{\mathcal{A}}\right)\right] = R\exp\left(K_D\left(\sigma_j^{\mathcal{A}}\sigma_k^{\mathcal{A}}+\sigma_k^{\mathcal{A}}\sigma_l^{\mathcal{A}}+\sigma_l^{\mathcal{A}}\sigma_j^{\mathcal{A}}\right)\right), \tag{19}$$

where R and K_D are two unknown parameters. What this physically means is that, we are replacing the interactions of the spin $\sigma_i^{\mathcal{B}}$ with each of the outer spins $\sigma_j^{\mathcal{A}}$, $\sigma_j^{\mathcal{A}}$, and $\sigma_j^{\mathcal{A}}$ individually, by the interactions among the outer spins alone. In the bond picture, the former looks like a star with three bonds coming out of $\sigma_i^{\mathcal{B}}$; the latter looks like a triangle connecting the outer spins. Accordingly, this maneuver is called the *Star-Triangle Transformation* or S.T.T.

Equation 19 is actually a set of eight equations, one for each spin combination of the three outer spins. Of these, only *two* are independent and yield two equations for R and K_D:

$$R = 2\cosh\left(\frac{3K}{4}\right)^{\frac{1}{4}}\cosh\left(\frac{K}{4}\right)^{\frac{3}{4}}, \tag{20}$$

$$K_D = \ln\left[\frac{\cosh\left(\frac{3K}{4}\right)}{\cosh\left(\frac{K}{4}\right)}\right]. \tag{21}$$

Using Equation 19 in our last expression for Z, we see that,

$$Z = R^N \sum_{\{\sigma_j^{\mathcal{A}}\}} \prod_{(j,k,l)} \exp\left(K_D\left(\sigma_j^{\mathcal{A}}\sigma_k^{\mathcal{A}}+\sigma_k^{\mathcal{A}}\sigma_l^{\mathcal{A}}+\sigma_l^{\mathcal{A}}\sigma_j^{\mathcal{A}}\right)\right), \tag{22}$$

where the product is over all the "downward-pointing" red triangles in Figure 3. Clearly, the summation in the above is nothing but the partition function of the triangular dual lattice, with N_D spins. Since $N_D = N/2$, scaling $N \to 2N$ and identifying $K = K$; $K_D = K_D$ allows us to rewrite the above as

$$Z(2N, K) = R^N Z_D(N, K_D), \tag{23}$$

which gives an exact mapping of the honeycomb lattice to its dual triangular lattice. Along with the expression for R, one can show that this is in fact equivalent to the duality relation (12) derived earlier.

2.4 The Critical Point

Having established this, we can now combine the ideas of duality and S.T.T. to infer the critical point of the honeycomb. First, we make use of an identity to exponentiate Equation 21 and rewrite it as

$$\exp\left(K_D\right) = 2\cosh\left(\frac{K}{2}\right) - 1. \tag{24}$$

This can now be compared directly to the reciprocal squared of Equation 10 that we derived earlier via duality:

$$2\cosh\left(\frac{K'}{2}\right) - 1 = \coth^2\frac{K}{4}, \tag{25}$$

where the prime index for now simply says we obtained K' in the context of duality. Using hyperbolic trigonometric identities and some algebra, we can put the above relation in a symmetric form:

$$\left[\cosh\left(\frac{K'}{2} - 1\right)\right]\left[\cosh\left(\frac{K}{2} - 1\right)\right] = 1. \tag{26}$$

This is analogous to Equation 10 in form but very different from it with regard to the physical meaning. Whereas Equation 10 maps a lattice to its dual lattice (or, a high-temperature model of Z to a low-temperature model of Z), Equation 26 maps the honeycomb to *itself*.

Nevertheless, the argument for identifying the critical point in both cases is similar. If K^* is a critical point, then so is K'^*, since they pertain to the same exact lattice. Hence, applying $K^* = K'^*$ in Equation 26, we finally obtain

$$\cosh^2\left(\frac{K^*}{2} - 1\right) = 1 \implies \tag{27}$$

$$\boxed{T^* \simeq 0.379663\,\frac{J}{k_B}.} \tag{28}$$

This is the critical temperature of the 2D spin-1/2 honeycomb lattice in the thermodynamic limit. In the next half, we report on our computer simulation of a honeycomb lattice to numerically derive this critical temperature.

3 Numerical Solution

To make our life simpler while doing the computer simulation, we transform the hexagonal lattice to a staggered square lattice, or a brick lattice (see Figure 4). While each spin at coordinate (i, j) has neighbors on the left and on the right, it has an upper (lower) neighbor only when $i + j$ is even (odd). Therefore, the total energy (Hamiltonian) of the brick lattice can be written as

$$E = -J\sum_{i,j=0}^{N}\begin{cases}\sigma_{i,j}\sigma_{i,j-1} + \sigma_{i,j}\sigma_{i,j+1} + \sigma_{i,j}\sigma_{i+1,j}, & (i+j) \bmod 2 = 0;\\ \sigma_{i,j}\sigma_{i,j-1} + \sigma_{i,j}\sigma_{i,j+1} + \sigma_{i,j}\sigma_{i-1,j}, & (i+j) \bmod 2 = 1.\end{cases} \tag{29}$$

Note that the brick lattice is equivalent to the honeycomb. The change here is not physically meaningful, unlike in the case of the Star-Triangle Transformation discussed previously. Rather, it is simply a trick to make it easier to label the lattice points in the computer code.

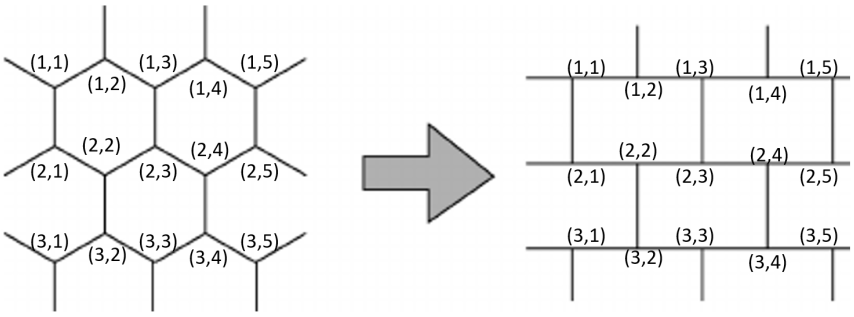

Figure 4: The transformation from a hexagonal lattice to a brick lattice. Coordinates of the lattice points are given in parentheses (Wakabayashi et al., 1999),

3.1 The Algorithm

In our numerical simulation, we apply the standard Metropolis-Hastings algorithm to simulate the spin states in the brick lattice, considering only nearest-neighbor interactions in no external magnetic field. We start with a brick lattice of 30×30 spins at some inverse temperature β, with each spin randomly assigned a value of $+1/2$ or $-1/2$. At every iteration, a spin is randomly chosen, and the energy cost δE to flip the spin to the opposite state is calculated. This energy cost is simply the difference in the energy of the lattice after and before flipping that particular spin, calculated using Equation 29. Then the flipping occurs as follows:

1. If $\delta E < 0$, flip the spin.
2. If $\delta E > 0$, flip the spin with probability $\exp(-\beta \delta E)$,

where the exponential factor comes from assuming our system is part of a canonical ensemble. We have also assumed here a periodic boundary condition, where the lattice wraps around on itself at the edges.

After a large number of iterations ($\sim 9 \times 10^6$), the total energy of the system stabilizes to its equilibrium value for that β. After that, we apply another set of iterations ($\sim 9 \times 10^6$) to derive various thermodynamic properties as ensemble averages:

$$\begin{aligned} M &= \sum_{i,j=0}^{N} s_{i,j}; \\ C &= \frac{1}{k_B T^2}(\langle E^2 \rangle - \langle E \rangle^2); \\ \chi &= \frac{1}{k_B T}(\langle M^2 \rangle - \langle M \rangle^2); \end{aligned} \tag{30}$$

where M is the magnetization, C is the specific heat, and χ is the magnetic susceptibility.

Next, we repeat the above process for a range of temperature values and plot the various thermodynamic quantities of interest listed above. More importantly, we look closely at the behavior of C and χ as a function of temperature, since a divergence in those quantities is the tell-tale sign of a phase transition in a planar lattice.

3.2 Simulation results

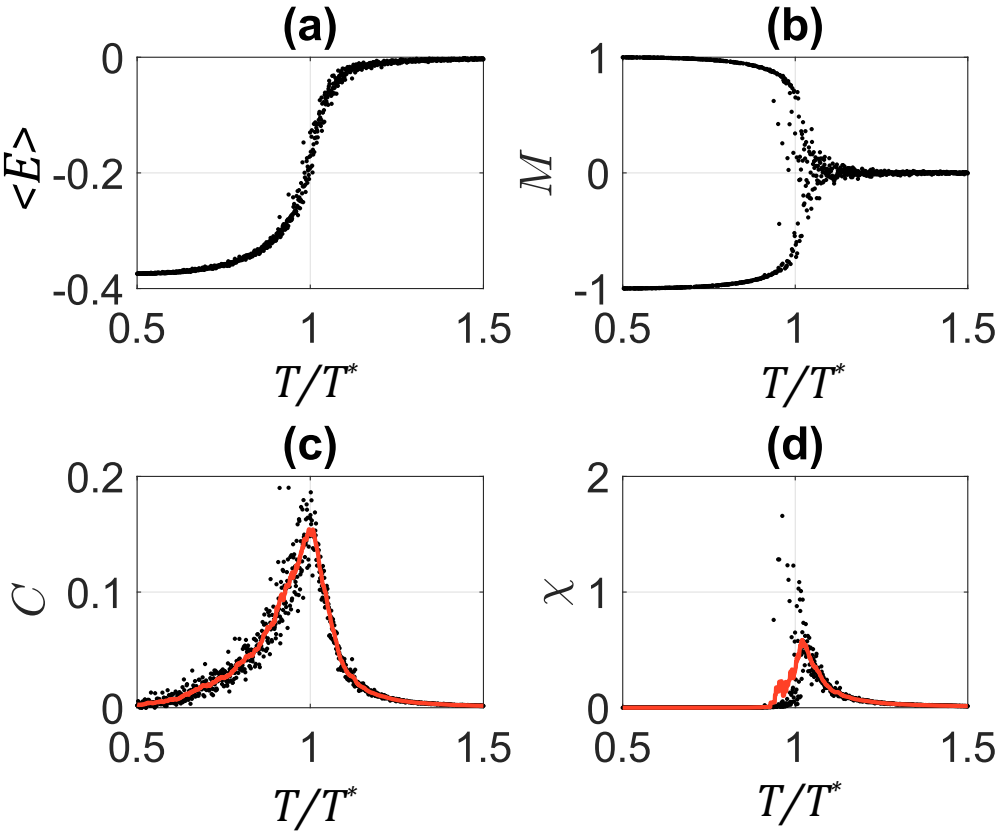

Figure 5: Results of the simulation for the honeycomb (brick) lattice. The black dots are the data points at various temperatures. $T^* = 0.3797J/k_B$ is the theoretical critical point. (a) The energy (in units of J) versus temperature. (b) The magnetization versus temperature. (c) The specific heat (in units of k_B) versus temperature. (d) The susceptibility versus temperature.

Here, we discuss the results of our numerical simulation, which are plotted in Figure 5. The y-axes are the various quantities of interest, whereas the x-axis is the temperature, normalized to the theoretical critical temperature $T^* = 0.3797J/(k_B)$ discussed in the previous section (Equation 28).

Looking at sub-graph (a), we see that the energy of the system starts out negative at low temperatures, where the spins tend to align all together to minimize the energy. The energy rises gradually until $T/T_c = 1$, where the slope of the curve increases dramatically. Similarly, from (b), the mean magnetization decays from ± 1 (fully magnetized) at low temperatures to almost 0 near the critical point, where it remains more or less constant. This means the spins transition from a fully-aligned state to a randomly distributed state after the critical point.

To extract the critical point from our simulation results, we look at the graphs of C and χ. From (c), we observe that C increases gradually from essentially 0 till a point where it seems to peak sharply. Past that point, it decreases in almost a symmetric manner down to 0 at high temperatures. We take the moving average of a few neighboring data points (black) and plot it continuously (red) to identify the peak. By choosing various numbers of neighboring data points, we derive a set of temperatures, whose standard deviation we take as the error. This way, we obtain $T^*_{\text{sim}} = 0.3785 \pm 0.0044 J/k_B$. This is very close to the theoretical value of $T^* = 0.3797 J/k_B$. In (d), we apply the same treatment to χ and get $T^*_{\text{sim}} = 0.3857 \pm 0.0040 J/k_B$, which also agrees very well with the expected value.

Further, it is also insightful to consider the spins themselves at the critical point and see how they "thermalize" after a number of Metropolis-Hastings iterations. In Figure 6, sub-graph (a) shows the spins in the brick lattice at the critical temperature in the initialization stage (zero iterations). Each site is randomly assigned a spin $+1/2$ or $-1/2$ (colors red and blue, respectively). Sub-graph (b) shows the system at 3×10^6 iterations – we see some clusters of red and blue spins forming. This is even more evident in (c) after 6×10^5 iterations – the clusters are now bigger in size on average. [2]

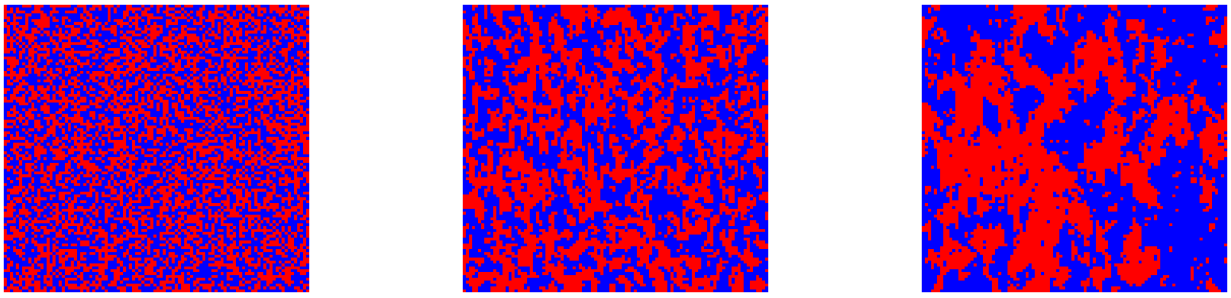

(a) (b) (c)

Figure 6: The spins in the 100×100 brick lattice after (a) 0, (b) 3×10^4 and 6×10^5 iterations at $T^* = 0.3797 J/k_B$. Cluster formation is evident after enough number of iterations (thermalization).

[2] The simulation codes are available at github.com/wonderingmark123/Ising-Model-Honeycomb

4 The Honeycomb with Defects

As a final task, we looked at the honeycomb lattice with two kinds of defect: (a) "holes" or missing spins and (b) impurities. These models simulate real-life crystals, which often have missing lattice points or foreign materials. Our intention was to look at the shift (if any) of the critical point in the presence of these defects.

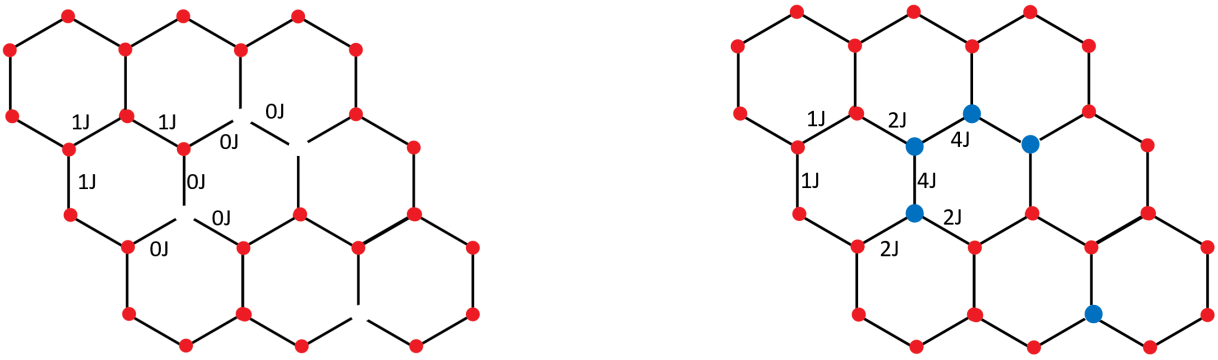

Figure 7: Defective Honeycomb. **[Left]** Lattice with missing spins where red dots are normal spins, and white dots represent "holes". **[Right]** Lattice with impurity, where red dots are normal lattice sites and blue dots represent impurities. The numbers shown here are the interaction strengths between neighbors.

For the holey honeycomb lattice, we randomly selected a proportion P of spins in our 30×30 brick lattice and set them to zero. These sites do not interact with their nearest neighbors at all and contribute nothing to the energy in Equation 29. Likewise, for the honeycomb with impurities, we again randomly selected a proportion P of lattice points and replaced them with "impure" spins with twice the numerical magnitude: $\sigma_i = \pm1/2 \rightarrow \sigma_i = \pm1$. Effectively, this modifies the interaction strength between two spins based on whether one or both or none of them are impure. The interaction strength of both missing spin and impurities is shown in Figure. 7

In the two cases, we varied P from 5% to 50%, and from 5% to 100% respectively, ran the Metropolis-Hastings algorithm, and obtained the critical point from the curves of C and χ. These results are plotted in Figure 8 as a function of P.

The figure shows interesting trends. In sub-figure (a), which plots the trend of the critical temperature as the proportion of missing spins in the lattice, the critical temperature as obtained from looking at χ decreases almost linearly with P (black dots). For the critical temperature as derived from C, the decrease is linear until $P = 25\%$, after which it is non-linear but still decreasing (red dots).

We are not sure why exactly the deviation from linearity in the latter case happens [3], but the linear downward trend has a simple explanation. As the number of holes in the lattice

[3] One possible reason for this is that P_{flip} at low temperatures is much smaller than at higher temperatures. This means that more iterations are needed in the former case.

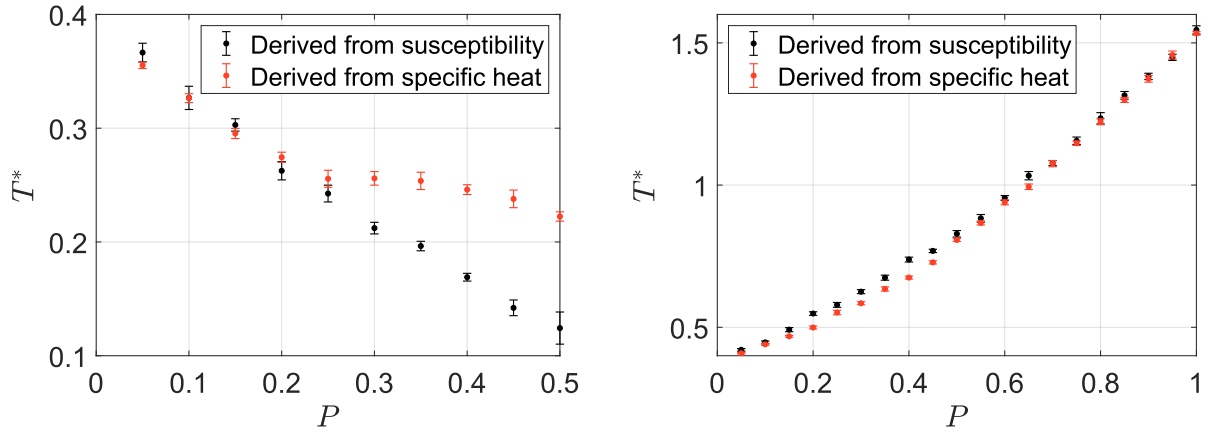

(a) (b)

Figure 8: Variation in the critical temperature due to missing lattice spins, (a), and due to impurities in the lattice, (b). The red dots are values derived from looking at C, whereas the black ones are from χ. Units on the y-axis are in J/k_B. For a "pure" lattice without any defects, $T^* = 0.379 J/k_B$.

increases, the effective average interaction J between any two spins in the lattice decreases proportionally. Accordingly, T^*, measured in units of J/k_B, decreases as well.

Similarly, looking at sub-figure (b) in Figure 8, we see a monotonic increase in the critical temperature as the proportion of impurities in the lattice is increased. Here, unlike in (a), we did not observe any significant deviation in the trend when looking at the red or the black data points. The upward increase also has an intuitive explanation. With the impurities interacting with greater strength than the regular spins, a higher concentration of impurities would increase the critical point. Accordingly, at $P = 1$, where every spin has been replaced by an impurity, the effective interaction strength is $4J$ among the spins, which means T^* rises to four times its value for a pure honeycomb, as confirmed by our plot.

5 Conclusion and Discussion

In this project, we derived the critical point of the honeycomb lattice in zero external field via theoretical considerations and verified it using numerical simulations. We also looked at the trend in the critical point in a defective honeycomb lattice – with holes and with impurities – and explained it by arguing its effect on the average interaction energy between spins.

To conclude, there are a few points about the numerical simulation that merit some discussion. The Metropolis-Hastings algorithm is very computationally-intensive and time-consuming. There are certain techniques that improve the speed of the algorithm – such as flipping an entire cluster of atoms in one iteration (Luijten, 2006), This is achieved, for

example, in the Swendsen-Wang algorithm and the Wolff algorithm. We did not, however, observe any significant improvement in our simulation with Wolff algorithm.

Secondly, our results of the critical temperature obtained from the graphs of C and χ deviate slightly from the theoretical value. This is understandable, since the latter is an exact result on an infinite lattice. We, on the other hand, used a lattice with 100×100 spins, which is far from the thermodynamic limit. Also important is the fact that we used a constant number of iterations at every temperature value (9×10^6). This number was picked to be as high as possible to ensure thermalization without slowing down the simulation too much; however the system might not always thermalize within this time, particularly near the critical point. This could affect our results as well.

Thirdly, there exist complicated analytical solutions for how the thermodynamic properties for a honeycomb lattice behave near the critical point. In particular, the specific heat is expected to increase logarithmically and symmetrically near the critical point (Houtappel, 1950):

$$C_c = \lim_{T \to T_c} \left[-\frac{C(T)}{k_B \ln\left(|T - T_c|\right)} \right]. \tag{31}$$

Unfortunately, we could not capture this logarithmic behavior in our results for C. We attribute this to the finite-size effect and the issue of finite number of iterations above.

Lastly, although no analytic solutions exist for the value of the critical point in the honeycomb in the presence of an external field B, this could easily be explored via numerical simulations by adding a magnetic interaction term in Equation 29.

References

Baxter, Rodney J. (1989). *Exactly Solved Models in Statistical Mechanics*. Academic Press Limited. ISBN: 0-12-083180-5.

Houtappel, Raymond Marie Ferdinand (1950). "Order-disorder in hexagonal lattices". In: *Physica* 16.5, pp. 425–455.

Luijten, E (2006). "Introduction to cluster Monte Carlo algorithms". In: *Computer Simulations in Condensed Matter Systems: From Materials to Chemical Biology Volume 1*, pp. 13–38.

Strečka, Jozef and Michal Jaščur (2015). "A Brief Account Of The Ising And Ising-like Models: Mean-field, Effective-field And Exact Results". In: *Acta Physica Slovaca* 65.4, pp. 235–367.

Wakabayashi, Katsunori, Mitsutaka Fujita, Hiroshi Ajiki, and Manfred Sigrist (Mar. 1999). "Electronic and magnetic properties of nanographite ribbons". In: *Phys. Rev. B* 59 (12), pp. 8271–8282. DOI: 10.1103/PhysRevB.59.8271. URL: https://link.aps.org/doi/10.1103/PhysRevB.59.8271.